Biochimica et Biophysica Acta, 471 (1977) 436—452

BBA 77875

OSMOTICALLY-INDUCED AND PHOTO-INDUCED DEFORMATIONS OF DISK MEMBRANES

TAKASHI NORISUYE * and HYUK YU

Department of Chemistry, University of Wisconsin, Madison, Wisc. 53706 (U.S.A.)

(Received March 3rd, 1977)

Summary

Effects of the osmotic pressure of suspending medium on the size and shape of isolated bovine rod outer segment disk membranes in the unbleached and bleached states were studied by elastic and quasielastic light scattering in dilute solutions of aqueous sucrose (0—0.1 wt.%). Data for the translational diffusion coefficients, D, and the elastically scattered intensities were analyzed with use of the oblate ellipsoidal shell model, and the axial ratio, ρ, and the major semi-axis, b, of the ellipsoid were deduced as a function of the concentration, c, of sucrose for each photochemical state (unbleached and bleached) of the membranes. The unbleached and bleached membranes suspended in water ($c = 0$) were found to be spherical vesicles, i.e., $\rho = 1$, of 0.49 μm radius. As c was increased, however, ρ for the bleached membranes rather steeply increased approaching 3 at $c = 0.1$ wt.%, whereas that for the unbleached membranes gradually increased (up to 2 at $c = 0.1\%$) after c exceeded 0.02%; at a fixed c, ρ increased upon bleaching. In all the cases, the deformation took place while b remained unchanged. The resulting contraction of the intravesicular volume induced either by the photo-bleaching or the osmotic pressure was accompanied by a significant decrease in the surface area of the membranes. The photo-induced contractions in the volume and the surface area amounted to 30—45% and 10—20%, respectively, in the concentration range from 0.02 to 0.1%. The dependence of D on c for each photochemical state was quantitatively explained by a simple model based on the Ca^{2+} efflux from the intravesicular space to the bathing medium upon bleaching.

Introduction

It is well-known that vertebrate rod outer segment disk membranes swell and contract in response to change in the osmotic pressure of bathing medium

* On leave from Department of Polymer Science, Osaka University, Osaka, Japan.

[1—3]. However, there exists no quantitative study of variation of the size and shape of the isolated rod outer segment disk membranes with the osmotic pressure. We report in this paper such a study performed with bovine rod outer segment disk membranes with focus on difference in osmotic behavior between two photochemical (unbleached and bleached) states. Dilute aqueous sucrose was chosen as the suspending medium because the membranes were expected to be impermeable to sucrose [1,2] and provided no indication for aggregation in this medium [4].

The membranes in native rod outer segment assume a thin disk shape, whereas those isolated by osmotic swelling are found to be spherical vesicles in a very low osmotic pressure medium such as water [5] or extremely dilute aqueous sucrose [6]. The thickness of the membranes has been shown to be quite small (approx. 75 Å) [7] compared to the radius of the disk (approx, 7500 Å) [8] or of the spherical vesicle (approx. 5000 Å) [5,6]. Thus, it seems reasonable to expect that the membranes in the intermediate stages between the native disk and spherical vesicle may be described by the model of oblate ellipsoidal shell. Given this model, the size and shape of the membranes are characterized by two parameters, the axial ratio, ρ, and the major semi-axis, b, of the ellipsoidal shell. In this work, we determine these parameters as a function of the concentration of aqueous sucrose for each photochemical state. The translational diffusion coefficients, D, obtained from quasielastic light scattering and the intensity profiles of elastically scattered light are analyzed with the aid of the corresponding theoretical equations; for the former we make use of Perrin's equation [9] and for the latter we derive the particle scattering function of oblate ellipsoidal shells. From the values of ρ and b so determined, we evaluate the volume and the surface area contractions of the vesicles induced by the photo-bleaching and the osmotic pressure of the suspending medium. Finally, the osmotic behavior of D characteristic of each photochemical state is discussed on the basis of the Hagins' model [10] of Ca^{2+} efflux from the intravesicular space upon bleaching.

Model and basic equations

Throughout this work, we assume the effect of optical anisotropy of the scattering elements to be negligible. It is based on our previous finding that the anisotropy effect can safely be ignored in the determination of the radius of membrane vesicles [6] and on the observation that the depolarized component of scattered intensity from any membrane suspension used in this work was quite small at any angle compared to the polarized component (the incident and scattered lights are both vertically polarized). Under the assumption of optical isotropy of the scattering elements, the particle scattering function, $P(x)$, of an oblate ellipsoidal shell is given by (see Appendix):

$$P(x) = \int_0^1 \frac{\sin^2[x(1-qt^2)^{1/2}]}{x^2(1-qt^2)}\,dt \tag{1}$$

with

$$q = 1 - \rho^{-2} \tag{2}$$

$$x = \kappa b \tag{3}$$

$$\kappa = (4\pi/\lambda') \sin(\theta/2) \tag{4}$$

where ρ is the axial ratio define as b/a ($\geqslant 1$) with the major semi-axis b and the minor semi-axis a, and κ is the magnitude of scattering vector with the wavelength of light λ' in the scattering medium and the scattering angle θ. The integration in Eqn. 1 is performed numerically at different values of x and ρ. Some of the results are graphically displayed in Fig. 1, where $x^2P(x)$ is plotted against x for various ρ. Characteristic features of this plot are that $x^2P(x)$ modulates in the range of x higher than 1.5 and that the modulation amplitude decreases with increasing ρ while the mean level of $x^2P(x)$ increases with ρ. Since the polarized scattered intensity $I_{vv}(\theta)$ from dilute solution is proportional to $P(x)$ and x is proportional to $\sin(\theta/2)$, the combined quantity $I_{vv}(\theta)\sin^2(\theta/2)$ is directly proportional to $x^2P(x)$. Hence, the values of $\sin(\theta/2)$ at which $I_{vv}(\theta)$-$\sin^2(\theta/2)$ reaches maximum or minimum correspond to x_{min} or x_{max}, the values of x, at which $x^2P(x)$ attains maximum or minimum and the relationship between $\sin(\theta/2)$ and x_{max} of x_{min} (Eqn. 3) allows us to evaluate b. We list in Table I the numerical values of x_{max} and x_{min} for different values of ρ. Excepting the first x_{max} and x_{min} values in the second and third columns of the table, any set of x_{max} or x_{min} is seen to be insensitive to ρ. Hence the determination of $\sin(\theta/2)$ at the extrema positions furnishes a ready estimate of b but not ρ. On the other hand, the asymptotic mean level or amplitude of $x^2P(x)$ at large x is a single valued function of ρ as can be seen in Fig. 1. Thus one can, in principle, deduce both b and ρ if the extrema positions, as well as the asymptotic mean level of $x^2P(x)$, can be determined experimentally. In practice, however, the absolute asymptotic mean value of $x^2P(x)$ is very difficult to determine; it requires the normalization of $I_{vv}(\theta)$ with respect to the intensity at zero angle, and this would entail measuring $I_{vv}(\theta)$ at extremely low angles and extrapolating to $\theta = 0$ (e.g. below 6° for $b = 5000$ Å and $\lambda' = 4000$ Å).

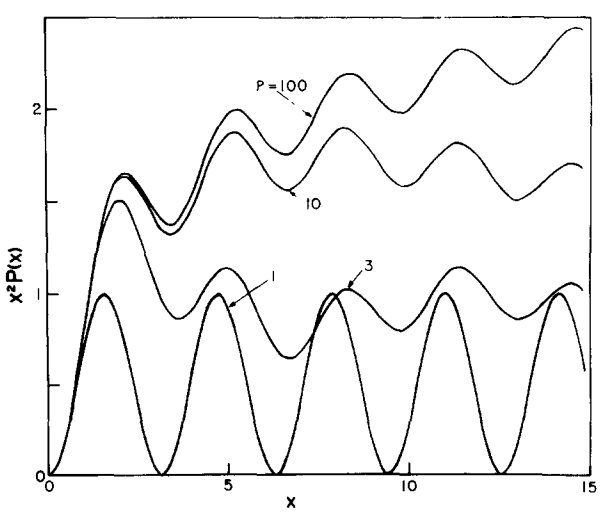

Fig. 1. $x^2P(x)$ for oblate ellipsoidal shell plotted against x for the indicated values of the axial ratio ρ.

TABLE I

NUMERICAL VALUES OF x AT THE EXTREMA OF $x^2P(x)$

ρ	x_{max} 1st	x_{min} 1st	x_{max} 2nd	x_{min} 2nd	x_{max} 3rd	x_{min} 3rd	x_{max} 4th	x_{min} 4th
1.0	$\pi/2$	π	$3\pi/2$	2π	$5\pi/2$	3π	$7\pi/2$	4π
1 2	1 66	3 33	4.99	6 64	8 28	9 91	11 5	13 1
1.4	1 74	3.47	5 17	6.82	8 37	9.81	11 3	12 9
1.6	1 80	3.57	5 26	6 77	8 17	9.71	11.4	13.0
1.8	1.85	3.64	5 25	6 63	8 14	9 82	11.5	13.0
2 0	1 89	3.68	5 18	6 56	8.21	9.91	11 4	12.9
2.2	1.92	3 69	5 11	6 56	8.28	9.91	11.3	12.9
2.4	1 95	3 69	5.05	6 59	8.33	9.86	11 3	13 0
2.6	1 97	3.69	5.01	6.63	8 35	9.79	11.3	13.0
2 8	1 99	3.68	4.99	6 67	8.35	9.75	11.4	13 0
3.0	2.01	3.67	4 98	6.71	8.33	9 73	11.4	13 0
5.0	2 10	3.52	5 05	6.78	8.15	9 88	11.4	12.9
10.0	2 15	3.43	5.17	6.66	8.24	9 86	11.3	13 0

To determine the two unknowns, b and ρ, we require another experimental quantity which depends on them. The translational diffusion coefficient, D is such a quantity. Since the model of oblate ellipsoidal shell should be hydrodynamically equivalent to that of oblate ellipsoid of revolution (see ref. 5), its translational diffusion coefficient is given by [9]:

$$D = \frac{kT\rho}{6\pi\eta b} G(\rho) \tag{5}$$

with

$$G(\rho) = \frac{\tan^{-1}(\rho^2 - 1)^{1/2}}{(\rho^2 - 1)^{1/2}} \tag{6}$$

where k is the Boltzmann constant, T the absolute temperature, and η the solvent viscosity. According to Eqns. 5 and 6, the experimental determination of D allows us to evaluate either b or ρ if the other one is known in advance.

Combining the experimentally determined values of D with the data for the extrema positions of $\sin^2(\theta/2)I_{vv}(\theta)$, one can deduce a unique set of the parameters characterizing the oblate ellipsoidal shell. In practice, we estimate b roughly from $\sin(\theta/2)$ at the extrema using a trial value of ρ and substitute the b value into Eqn. 5 to determine ρ. A newly determined value of ρ is then used to obtain b with the aid of the tabulation. The iterative procedure is continued until a self-consistent set of b and ρ are obtained. Because of the insensitivity of the extrema positions on ρ (see Table I), the trial choice of ρ is immaterial and only a few iterations would suffice.

Materials and Methods

Bovine rod outer segment disk membranes were isolated and purified by the method of Smith et al. [11]. Elastic light-scattering measurements were performed on a SOFICA photogoniometer (Bausch and Lomb; Model 40000)

at room temperature. The incident light (546 nm wavelength) and scattered light were both vertically polarized with respect to the scattering plane. For the unbleached membranes, effects of the exposure to the green light, which would result in bleaching of rodopsin, was examined with use of a light scattering cell having a Teflon insert which was so designed that the incident beam (approximetaly 0.2 cm in width and 1 cm in height) was made to illuminate the whole of a membrane suspension in the cell. Absorbances ($A_{498\,nm}$) were measured before and after the exposure. The results showed a roughly linear decrease in $A_{498\,nm}$ of 5% per 10 min over a period of 30 min. A 2% decrease in $A_{498\,nm}$ was observed for the first 5 min, which implied that effects of the exposure on elastic light-scattering data could safely be ignored for this period. In fact, $I_{vv}(\theta)$ did not change within the first 5 min when measured in $2.50 \cdot 10^{-2}$% aqueous sucrose at $\theta = 81°$. Inasmuch as our purpose is to determine $\sin(\theta/2)$ at maxima or minima of $\sin^2(\theta/2)I_{vv}(\theta)$, this period was sufficient to obtain the value of $\sin(\theta/2)$ at one of the extrema. Thus, $I_{vv}(\theta)$ for the unbleached membrane suspensions was monitored at 1° increments in the angular range of 63–73° and all the measurements were completed within 5 min. For the bleached membrane suspensions, on the other hand, the measurements were made over an angular range of 30–140°. The same experimental procedures as described previously [6] were employed for both the unbleached and bleached membranes. The variability of b determined from different $\sin(\theta/2)$ values at different maximum and minimum positions of $\sin^2(\theta/2)I_{vv}(\theta)$ was estimated in terms of the two standard deviations to give ±2–5% for each of bleached membrane suspensions. We can infer a similar uncertainty of b for the unbleached membranes although the error could not be estimated because b was determined from single maximum position.

Quasielastic light-scattering measurements were made at room temperature (25.1 ± 0.1°C) with the unpolarized light of 3 mW He-Ne laser (632.8 nm; Spectra Physics 135). The same apparatus and procedures as in previous studies [4,6] were used; the single Lorentzian halfwidth at half height $\Delta\nu_{1/2}$ of the scattered spectrum was obtained as a function of θ and D was determined from the slope of a plot of $\Delta\nu_{1/2}$ vs. κ^2/π where κ is defined by Eqn. 4. The estimated uncertainties of D arising from determinations of the slope by the least-square analysis with Student's t-distribution [12] was +3–9% within the 95% confidence limits.

The osmotic pressure of suspending medium was varied by changing the concentration of sucrose from 0 to 0.1 wt.%. An independently prepared suspension was used for each elastic or quasielastic light-scattering measurement. In higher concentrations (3–10%) of sucrose, the membranes appeared to aggregate. We thus confined ourselves to study in a relatively low concentration region of sucrose.

Results and Discussion

Elastic scattering profiles

The elastic light scattering data for the unbleached and bleached membranes in aqueous sucrose are displayed in Fig. 2, where $\sin^2(\theta/2)I_{vv}(\theta)$ is plotted against $\sin(\theta/2)$ corresponding to $x^2P(x)$ vs. x plots in Fig. 1. As expected, the

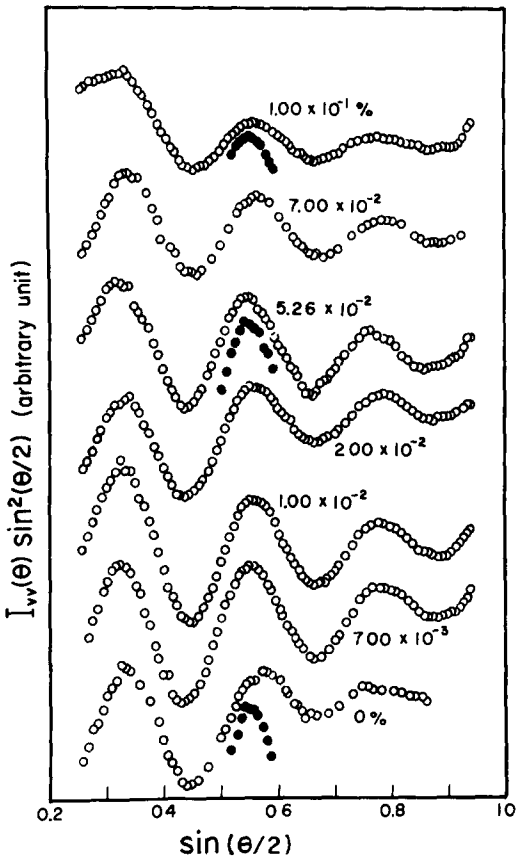

Fig. 2. Plots of $\sin^2(\theta/2)I_{VV}(\theta)$ vs. $\sin(\theta/2)$ for isolated bovine rod outer segment disk membranes in aqueous sucrose of the indicated concentrations. ●, Unbleached membranes, ○, bleached membranes.

scattering profile for each suspension is seen to modulate. The extrema position in all the profiles appear at approximately the same set of scattering angles, indicating that the major axis, b, of the membranes is roughly the same regardless of the photochemical state of the membranes and the concentration of sucrose. The correspondence of the observed first maximum to the second maximum in the theoretical profile is ascertained by trial matching of the whole experimental curve at $c = 0$ (pure water) to the theoretical one at $\rho = 1$ and by obtaining a consistent radius. Once the correspondence is established, the initial value of b is readily determined; since the observed extrema positions appear at about the same scattering angles for all the suspensions, the value of $b = 0.47$ μm thus obtained at $c = 0$ would serve as the initial trial one for all cases.

Diffusion coefficients

The angular dependence of $\Delta\nu_{1/2}$ for the unbleached membranes in aqueous sucrose is displayed in Fig. 3 and the corresponding plot for the bleached membranes is shown in Fig. 4. The data points for each photochemical state of the membranes in different sucrose concentrations follow respective straight lines.

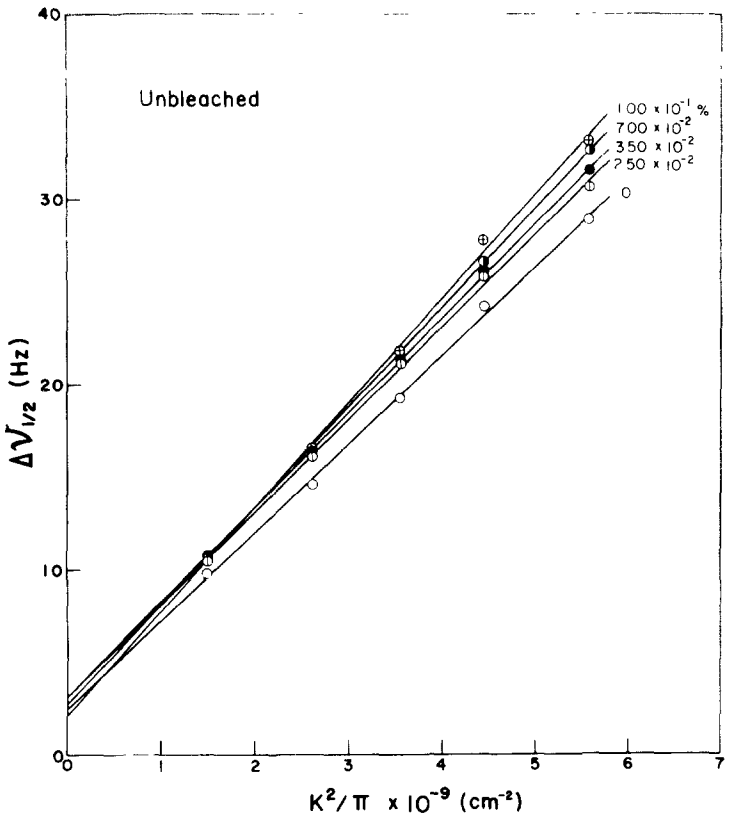

Fig. 3. Plots of the spectral halfwidth at half-height $\Delta\nu_{1/2}$ vs. κ^2/π for the unbleached membranes in aqueous sucrose of the indicated concentrations.

The translational diffusion coefficients, D, calculated from the slopes (see ref. 4 for the significance of intercepts) are collected in Table II together with the measured viscosity η of each suspension. The diffusion coefficients $D_{20,w}$ reduced to the viscosity of water at 20°C by the relation, $D_{20,w} = D(\eta/1.00)(293.2/298.2)$, are also given in Table II. In Fig. 5, we plot $D_{20,w}$ against sucrose concentration c (in units of wt.%); the significance of the solid curves is discussed below. Features of the two sets of data points may be summarized as follows: (1) $D_{20,w}$ for the unbleached membranes is essentially the same as for the bleached membranes in pure water (or at very small c); (2) $D_{20,w}$ for the bleached membranes increases rather sharply with c at the beginning followed by a gradual increase; (3) $D_{20,w}$ for the unbleached membranes increases very gradually or even appears to stay constant until c exceeds approx. 0.02%, and (4) $D_{20,w}$ for the unbleached membranes is consistently lower (by about 10%) than that for the bleached membranes at the same c except when c is very small. We infer from the last observation that the membranes contract upon bleaching. The values of $b/\rho G(\rho)$ calculated with use of Eqn. 5 are given in Table III. Note that when the membranes are spherical vesicles, $b/\rho G(\rho)$ equals to the Stokes radius.

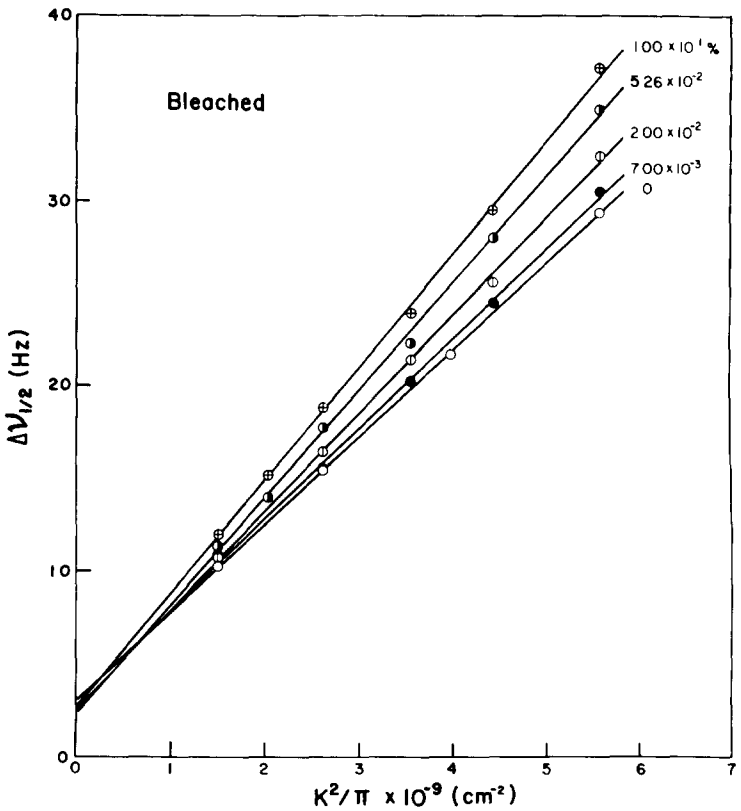

Fig. 4. Plots of $\Delta\nu_{1/2}$ vs. κ^2/π for the bleached membranes in aqueous sucrose.

Paremeters of oblate ellipsoidal shell model

Following the analysis scheme outlined above, we extract b and ρ from the data of $D_{20,w}$ and $\sin(\theta/2)$ at the extrema in the $\sin^2(\theta/2)I_{vv}(\theta)$ vs. $\sin(\theta/2)$

TABLE II

TRANSLATIONAL DIFFUSION COEFFICIENTS FOR ISOLATED BOVINE ROD OUTER SEGMENT DISK MEMBRANES IN AQUEOUS SUCROSE

Concentration of sucrose (wt%)	Unbleached			Bleached		
	$D \times 10^9$ (cm^2/s)	η (centipoise)	$D_{20,w} \times 10^9$ (cm^2/s)	$D \times 10^9$ (cm^2/s)	η (centipoise)	$D_{20,w} \times 10^9$ (cm^2/s)
0	4 77	0.927	4 35	4.69	0.915	4.22
$4.36 \cdot 10^{-3}$ *	4.19	1.03	4.25	4.19	1 03	4 25
$7.00 \cdot 10^{-3}$	—	—	—	4.84	0.961	4.58
1.00 10^{-2}	—	—	—	5.47	0.914	4.92
2.00 10^{-2}	4.67	0.956	4 39	5.28	0.961	4.99
$2.50 \cdot 10^{-2}$	5.00	0.913	4.49	—	—	—
$3.50 \cdot 10^{-2}$	5.09	0.948	4.74	—	—	—
$5.26 \cdot 10^{-2}$	5.15	0.956	4.84	5.79	0.961	5.47
$7.00 \cdot 10^{-2}$	5.43	0.927	4 95	6.08	0.961	5.74
$1.00 \cdot 10^{-1}$	5.63	0.977	5.41	6.12	0.960	5 78

* Taken from our previous data [4,6].

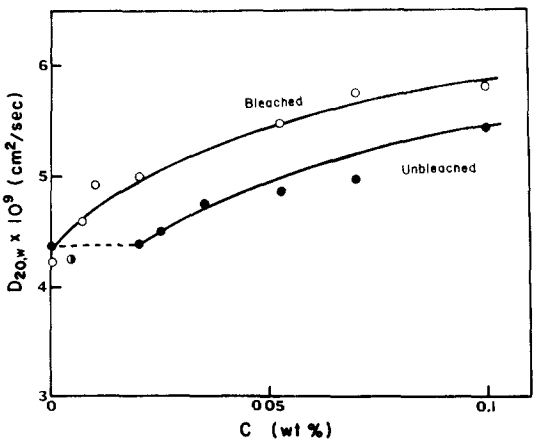

Fig. 5. The reduced translational diffusion coefficients, $D_{20,w}$ are plotted against the concentration of sucrose, c (wt.%). ●, for the unbleached membranes, ○, for the bleached membranes, and ◑ is taken from our previous data for both the unbleached and bleached membranes [4,6]. The solid curves are drawn with $\alpha = \alpha_b = 3.5 \cdot 10^{-5}$ cm^2/dyne (see text).

curves by successive interations; two iterations are sufficient to deduce the final set of b and ρ for each suspension. The results are summarized in Table III. We first note that the data for the unbleached membranes in pure water and c at 0.02%, and 0.025%, and for the bleached membranes in pure water yield $\rho = 1$. Therefore, the values of $b/\rho G(\rho)$ and b for these suspensions are regarded, respectively, as the Stokes radius and the equilibrium radius of the spherical vesicles. The agreement among these sets of radii (0.51—0.47 μm) confirms the previous findings [6] that the Stokes radius is equivalent to the equilibrium radius and that the radius of the spherical vesicles is 0.49 ± 0.07 μm. Secondly, it may be noted that since the function $G(\rho)$ (Eqn. 6) is rather insensitive to ρ, particularly at larger values of ρ, the precision for determinations of ρ values is poor. Nevertheless, it can clearly be seen that, while b stays almost constant (0.47—0.50 μm) ρ increases with increasing c or upon bleaching; in other words, the membrane deformation takes place in such a way that only the minor axis contracts. This anisotropic deformation (shown schematically in Fig. 6) suggests the existence of a certain rim effect. Such a rim effect could arise if the structural constituents are different from the rest of a disk membrane or the packing density of intramembraneous components is greater in the equatorial plane corresponding to the circumference of a native disk adjacent to the plasma membrane [13—15]. Thus, the anisotropic deformation may furnish further information of the membrane structure. On the other hand, the difference between the value of b approx. 0.5 μm for isolated membrane vesicles and 0.75 μm for the radius of the native disks [8] is hard to account for unless b can increase at some point beyond the range of ρ that we have examined. In this regard, the dimension of rod outer segment reported by McConnell [8] should be restudied.

Volume and surface area contractions

Once the values of b and ρ are determined, we can calculate the volume V

TABLE III

PARAMETERS OF OBLATE ELLIPSOIDAL SHELLS FOR ISOLATED BOVINE ROD OUTER SEGMENT DISK MEMBRANES

Concentration of sucrose (wt.%)	Unbleached					Bleached				
	$b/\rho G(\rho)$ (μm)	b (μm)	ρ	V (μm^3)	A (μm^2)	$b/\rho G(\rho)$ (μm)	b (μm)	ρ	V (μm^3)	A (μm^2)
0	0.49	0 47	1.0	0.46	2 9	0.51	0 47	1.0	0.49	3 0
$4.36 \cdot 10^{-3}$	0 51	0 48	1.0	0.51	3 1	0.51	0.48	1 0	0.51	3.1
$7.00 \cdot 10^{-3}$	—	—	—	—	—	0.47	0.48	1 05	0.44	2 7
$1.00 \ 10^{-2}$	—	—	—	—	—	0.44	0.49	1.5	0.33	2.4
$2.00 \cdot 10^{-2}$	0.49	0.48 *	1 0	0.48	3.0	0.43	0 49	1.5	0.33	2.4
$2.50 \cdot 10^{-2}$	0 48	0.47	1.0	0.45	2 8	—	—	—	—	—
$3.50 \cdot 10^{-2}$	0.45	0.50 *	1 3	0.40	2.6	—	—	—	—	—
$5.26 \cdot 10^{-2}$	0.44	0.49	1.4	0.35	2.5	0.39	0.49	2.4	0.21	2.0
$7.00 \cdot 10^{-2}$	0.43	0.49 *	1.6	0 31	2 3	0.37	0.47	2.5	0.17	1 8
$1.00 \cdot 10^{-1}$	0.40	0.48	2.0	0.23	2.0	0.37	0.48	2.9	0.16	1.8

* Calculated by assuming the $\sin(\theta/2)$ value at maximum of $\sin^2(\theta/2)I_{VV}(\theta)$ is the same as in other sucrose concentrations and with the same analysis scheme outlined in the text

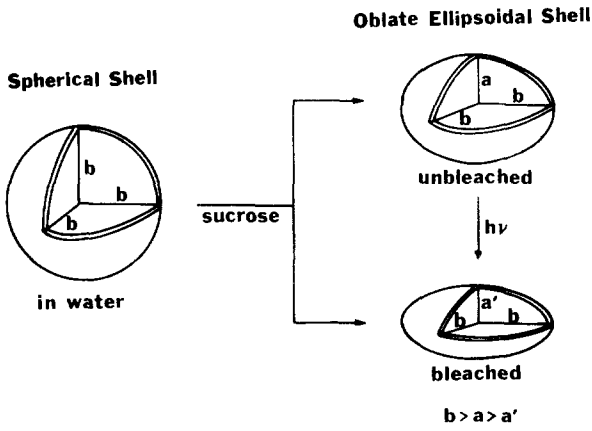

Fig. 6. Schematic presentation of osmotically-induced and photo-induced deformations of bovine rod outer segment disk membranes. b and a (or a') denote, respectively, the major and minor semi-axes of oblate ellipsoidal shell.

and the total surface area A of the membrane vesicles by the following expressions for the oblate ellipsoid of revolution:

$$V = \tfrac{4}{3}\pi b^3 \rho^{-1} \tag{7}$$

$$A = 2\pi b^2 \left[1 + \frac{1}{2\rho^2\sqrt{1-\rho^{-2}}} \ln \frac{1+\sqrt{1-\rho^{-2}}}{1-\sqrt{1-\rho^{-2}}}\right] \tag{8}$$

The values of V and A so calculated are listed in Table III. At the same concentration of sucrose ($0.02\% \leqslant c \leqslant 0.1\%$), the volume of the vesicles contracts upon bleaching by 30—45%. This photo-induced volume decrease is more pronounced than that (12—15%) observed by Heller et al. [16] for frog rod outer segment. The photo-induced decrease in A on the other hand, amounts to 10—20% in the range of $0.02 \leqslant c \leqslant 0.1\%$, indicating that an average distance between a pair of nearest neighbors of intramembraneous components decreases by 5—10% upon bleaching. This decrease is compared favorably with the decrease of 5—9% in the average distance between two adjacent photopigments found by Blasie [17] by the X-ray diffraction with isolated frog rod outer segment disk membranes.

We have previously reported that D for the membranes in 5% aqueous Ficoll increased upon bleaching [4]. The photo-induced decreases in V and A were evaluated by assuming that the shape of the vesicles was spherical either in the unbleached or bleached state. However, the present analysis shows that any isotropic contraction (with the spherical shape intact) does not occur in aqueous sucrose. Since Ficoll is a polymer of sucrose, an anisotropic deformation similar in sucrose would be expected for the vesicles in aqueous Ficoll. Therefore, the previous estimates of the photo-induced changes in volume and surface area must be accepted with reservation until detailed information of the shape in Ficoll becomes available.

Osmotic behaviors

We have demonstrated that the isolated rod outer segment disk membranes

deform and contract as the concentration of sucrose, c, in the suspending medium is increased. The deformation takes place while the major axis remains unchanged. A remarkable difference of the osmotic behaviors in the unbleached and bleached states is that the axial ratio in the bleached state increases steeply at small c while that in the unbleached state increases very gradually or even stays at unity until c exceeds $2 \cdot 10^{-2}$%. Beside this qualitative difference, the vesicular volume in either the bleached or unbleached state does not follow a simple functional relationship with respect to c such as c^{-1} dependence; this can be seen easily from the data collected in Table III. One might have expected such a dependence if the membranes were perfectly flexible and the osmotically active solutes within the intravesicular space remained conserved while c was varied such that the vesicles would deform (and contract) until there existed no osmotic pressure across the membranes, i.e., the chemical potential of the sole, permeable component (H_2O) equalized. We find from the data in Table III that the progression of vesicular deformation is less sensitive than c^{-1} incremental change. We, therefore, suspect that the membranes are capable of sustaining a finite osmotic pressure Π, at any c away from the isotonic condition. Such situations would arise if the membranes are not completely flexible and Π, the pressure gradient across them, is compensated by the surface tension. In the following, an attempt is made to interpret the osmotic behaviors in terms of a simple model. The task is to find an explanation of the observed qualitative difference between the two photochemical states and to explain the vesicular volume dependence on c in their respective photochemical states.

Our model is entirely based on the assumption that in the intravesicular space of the membrane there exist osmotically active ions which contribute to the chemical potential of water. For simplicity, we take these ions to be Ca^{2+} and univalent anions whose concentration equivalence to Ca^{2+} is maintained by electroneutrality. We further assume that the membrane in the unbleached state is impermeable to Ca^{2+} with negligible leakage, whereas Ca^{2+} permeability in the bleached state is completely symmetric across the membranes. These assumptions are based on Hagins' model [10] which supposes that the Ca^{2+} efflux from intradiskal to extradiskal direction is photo-induced [18—23]. Thus, our system is composed of the membrane vesicles, sucrose, H_2O, Ca^{2+}, and the accompanying anions. The membranes are assumed to be impermeable to sucrose [1,2] and the concentrations of sucrose and ions are such that their activity coefficients are assumed to be unity. With this decription of the model, we can readily find the expressions for the osmotic pressure.

In the unbleached state,

$$\Pi = RT\left(\frac{10^{-2}c}{M_s} - 3 \cdot 10^{-3}m\right) \tag{9}$$

$$= RT\left(\frac{10^{-2}c}{M_s} - \frac{3 \cdot 10^{-6}n}{V}\right) \tag{9a}$$

and in the bleached state,

$$\Pi = RT\left(\frac{10^{-2}c}{M_s} - 3 \cdot 10^{-3}\Delta m\right) \tag{10}$$

where RT has the usual meaning, M_s is the molecular weight of sucrose, c is sucrose concentration in units of weight percent in water, m and n are, respectively, the molar concentration and the mole number of Ca^{2+} within a vesicle in the unbleached state, V is the corresponding vesicular volume in cm^3, and Δm is the molar concentration difference of Ca^{2+} between the ones inside and outside of a vesicle in the bleached state. In arriving at Eqns. 9 and 10, we assumed the density of water to be 1 g/ml and made use of an approximation, $\ln(1 - X_2) \approx -X_2$ when $X_2 << 1$, since sucrose and ionic concentrations (see below) are all small enough. With these two equations, we are now able to provide explanations for the different features of the osmotic behaviors in the two photochemical states.

Eqn. 9 indicates that (1) the isotonic condition across the membranes is $c^* = 0.3\ M_s m$ and (2) Π becomes negative when c decreases below c^*. In such instances, the chemical potential of H_2O in the extravesicular solution is greater than in the intravesicular solution which will result in further swelling of the vesicles beyond the dimension at the isotonic condition until the chemical potential equalizes. This can take place only if the membranes are stretchable without limit. The observed constancy of the vesicular volume and preservation of spherical shape for $0 \leqslant c \leqslant 0.02\%$ (within the experimental uncertainty) are clearly contrary to this expectation. Thus, we hypothesize that the vesicles remain at their maximum extent of swelling for $0 \leqslant c \leqslant 0.02\%$ and any decrease in c below c^* would either induce bursting of the vesicles or have no effect on the size and shape. Increase in c beyond c^*, on the other hand, results in deformation of the spherical vesicles into the oblate ellipsoidal shells. On this basis, we can calculate the molar concentration of Ca^{2+} within a vesicle in the unbleached state. From the isotonic condition, $m = c^*/0.3\ M_s$, we find $m = 2 \cdot 10^{-4}$ M if $c^* = 0.02\%$. From the value of vesicular volume at c^*, n in Eqn. 9a can be calculated as 10^{-19} mol, corresponding to $6 \cdot 10^4$ calcium ions per membrane.

In the bleached state, Eqn. 10 indicates that the isotonic condition depends on the molar concentration difference of Ca^{2+} between inside and outside of a vesicle Δm. Since the chemical potentials of Ca^{2+} and the accompanying univalent anions must be equalized in the bleached state while the extravesicular solution volume is about 100-fold of the intravesicular volume, we can safely write $\Delta m \approx 0$ if we accept m being of the order of 10^{-4} M. Then, Eqn. 10 is approximated as

$$\Pi \approx \frac{cRT}{10^2 M_s} \quad \text{(bleached)} \tag{11}$$

The isotonic state given by this equation is $c^* = 0$. Thus, the starting point of deformation profile of the bleached membranes requires no critical sucrose concentration. This would explain the difference in qualitative features of the plots shown in Fig. 5.

We now turn to the deformation behaviors of the vesicles with respect to c. We start by regarding the membrane surface to be a two-dimensional continuum with photopigments distributed uniformly over the entire closed surface. The focus is to relate the observed axial ratio ρ to the independent variable c. The previous discussions on the isotonic condition and the vesicular shape can be compactly stated as $\rho = 1$ for $\Pi \leqslant 0$. At the other extreme of the

native disk shape, Heller et al. [1] found that the disk volume in frog rod outer segment increased in inverse proportion to solute concentration of the suspending medium. This means that $\rho \propto \Pi$ for $\rho >> 1$ because $V \propto \rho^{-1}$ (from Eqn. 7 at constant b) and $\Pi \propto c$. Combining the two limits, we arrive at

$$\rho = 1 + \alpha\Pi \quad \text{for } \Pi \geqslant 0 \tag{12}$$

where α, formally given by $(\partial\rho/\partial\Pi)_T$, may be regarded as constant for a small range of Π and can be taken as a measure of the membrane stiffness. If the membrane bilayer thickness, l, is not affected by the osmotic pressure of bathing medium, as found by Korenbrot et al. [3], $(\partial\rho/\partial\Pi)_T$ can be related to the compressional modulus γ of the membrane by

$$\gamma^{-1} = -\frac{1}{v}\left(\frac{\partial v}{\partial \Pi}\right)_T = \frac{2}{\rho(\rho+2)}\left(\frac{\partial \rho}{\partial \Pi}\right)_T \tag{13}$$

where v is the shell volume per vesicle and given by

$$v = \tfrac{4}{3}\pi l b(b + 2a) \quad (b \geqslant a \gg l) \tag{14}$$

Thus, the parameter α is inversely proportional to the compressional modulus γ at a given axial ratio; the smaller is α, the stiffer the membrane. By substituting Eqn. 12 into Eqn. 9a with $n = 10^{-19}$ mol and $b = 4.9 \cdot 10^{-5}$ cm for $V = 4\pi b^3/3\rho$ (Eqn. 7), we obtain

$$\rho = \frac{1 + 10^{-2} M_s^{-1} \alpha RTc}{1 + 6 \cdot 10^{-7} \alpha RT} \quad \text{for } c \geqslant 0.02\% \text{ (unbleached)} \tag{15}$$

for the unbleached state. Combining Eqns. 11 and 12, we come to

$$\rho = 1 + 10^{-2} M_s^{-1} \alpha_b RTc \quad \text{(bleached)} \tag{16}$$

where α_b refers explicitly to the bleached state. These equations represent the desired relationships between the experimental quantity ρ to the independent variable c, and with the aid of them we can perform single-parameter analysis of the deformation behaviors of membrane vesicles at their respective photochemical states. With the data of ρ and c in Table III, we first calculated $\alpha = (3 \pm 1) \cdot 10^{-5}$ and $\alpha_b = (4 \pm 1) \cdot 10^{-5}$ cm^2/dyne, respectively, for the unbleached and bleached state. In view of uncertainties associated with determinations of ρ, we can scarcely claim these values to be different. Thus, within the experimental uncertainty of our measurements, the membrane stiffness is concluded to be about the same in the unbleached and bleached state. With $\alpha = \alpha_b = 3.5 \cdot 10^{-5}$ cm^2/dyne, we can now relate the primary experimental quantity D to c because D is a function only of ρ (given that b is constant), as given in Eqn. 5. The profiles of D with respect to c thus calculated are drawn in Fig. 5. The experimental data are well represented by these curves. The different behaviors of $D_{20,w}$ for the unbleached and bleached membranes are to a large extent, accounted for by Ca^{2+} efflux attendant difference in the osmotic pressure. Though not shown here, another set of α values ($\alpha = 3 \cdot 10^{-5}$ and $\alpha_b = 4 \cdot 10^{-5}$ cm^2/dyne) gave a better agreement between the experiment and the single parameter prediction. This might be taken as an indication that the membranes in

the unbleached state are stiffer than those in the bleached state at a given value of ρ. Such a definitive analysis, however, seems inconsistent in the context of the present work. We might add parenthetically that the compressional modulus of 10^5 dyne/cm^2, estimated from the α value is to be compared with the Young's modulus of 10^6–10^7 dyne/cm^2 for crosslinked rubbers [24].

In summary, the dependence of D on sucrose concentration for each photochemical state can be explained quantitatively by the simple model based on Hagins' hypothesis for native disks [10]. This indicates that the data of D for the isolated membranes are consistent with Hagins' model, although the ions assumed in the present analysis does not necessarily have to be Ca^{2+}. Our nontrivial assumption for the existence of certain ions which, upon bleaching, efflux from the intravesicular space is, however, to be verified experimentally. An investigation to estimate the concentration of such ions (actually Ca^{2+}) is now in progress in this laboratory.

Appendix

In this appendix, we calculate the particle scattering function $P(x)$ for an oblate ellipsoidal shell. Assuming that the scattering elements are optically isotropic and distribute uniformly over the surface of the ellipsoid, $P(x)$ is given by [25].

$$P(x) = \text{const.} \int Q^2 \mathrm{d}\Omega \tag{A-1}$$

with

$$Q = \int_{\text{surface}} e^{i\underset{\sim}{\kappa} \cdot \underset{\sim}{r}} \, \mathrm{d}\underset{\sim}{r} \tag{A-2}$$

where $\underset{\sim}{\kappa}$ is the scattering vector whose magnitude is given by Eqn. 4 and $\underset{\sim}{r}$ is the vector from a point on the surface to the origin of the coordinate which is fixed at the center of mass of the ellipsoidal shell. The integral in Eqn. A-2 must be performed over the surface of the ellipsoid in a given orientation Ω and the integral in Eqn. A-1 refers to the average over all the possible orientation of the ellipsoidal shell. For convenience, we choose the direction of $\underset{\sim}{\kappa}$ as the z-axis in the laboratory-fixed Cartesian system (x, y, z) and define a coordinate system (ξ, η, ζ) fixed in the ellipsoidal shell so that the direction of the semi-minor axis, a, is in the ξ axis. Letting α and β be, respectively, the angle between z and ζ axes and the angle between ξ axis and the projection of the z-axis on the η-ξ plane, Eqn. A-2 can be rewritten in terms of the coordinate system (ξ, η, ζ) as

$$Q = \int_{\text{surface}} \int \int e^{i\kappa(\xi \sin\alpha \cos\beta + \eta \sin\alpha \sin\beta + \zeta \cos\alpha)} \, \mathrm{d}\xi \, \mathrm{d}\eta \, \mathrm{d}\zeta \tag{A-3}$$

The surface integral of this equation is bounded by the relation

$$\frac{\xi^2}{a^2} + \frac{\eta^2}{b^2} + \frac{\zeta^2}{b^2} = 1 \tag{A-4}$$

for the ellipsoid of revolution with the semi-major axis, b, and the semi-minor axis, a. Writing $\xi = aX$, $\eta = bY$, and $\zeta = bZ$, we have

$$Q = ab^2 \int\int\int_{X^2+Y^2+Z^2=1} e^{ix[\rho^{-1}X \sin\alpha \cos\beta + Y \sin\alpha \sin\beta + Z\cos\alpha]}\, dX\, dY\, dZ \tag{A-5}$$

with the axial ratio ρ ($= b/a$) and x defined by κb (Eqn. 3). Transforming the (X, Y, Z) coordinate system into the polar coordinates with the aid of Poisson's formula [26], i.e.,

$$\int_0^{\pi} [\int_0^{2\pi} f(a\cos\theta + b\sin\theta\cos\phi + c\sin\theta\sin\phi)\sin\theta\, d\phi]\, d\theta$$

$$= 2\pi \int_{-1}^{1} f(\sqrt{a^2+b^2+c^2}x)\, dx$$

We can evaluate the integral in Eqn. A-5 as

$$Q = 4\pi ab^2 \frac{\sin[x(1-q\cos^2\alpha)^{1/2}]}{x(1-q\cos^2\alpha)^{1/2}} \tag{A-6}$$

where q is defined by Eqn. 2. Finally, substitution of Eqn. A-6 into Eqn. A-1, followed by normalization, yields Eqn. 1. When $\rho = 1$, Eqn. 1 reduces to the correct limit of spherical shell

$$P(x) = \left(\frac{\sin x}{x}\right)^2 \tag{A-7}$$

Eqn. 1 also holds for the prolate ellipsoid shell model if q and x are replaced by $-q$ and κa, respectively. We might add that the integral of Eqn. 1 can be evaluated exactly by expanding the integrand in a power series of x. The result is

$$P(x) = \frac{\sqrt{\pi}}{2} \sum_{n=0}^{\infty} \frac{(-1)^n x^{2n}}{\Gamma(n+\frac{3}{2})\Gamma(n+2)}\ {}_2F_1(-n, \tfrac{1}{2}; \tfrac{3}{2}; q) \tag{A-8}$$

where Γ and ${}_2F_1$ denote, respectively, the Gamma function and the hypergeometric function [27]. This equation is useful, however, only for small values of x.

Acknowledgement

We acknowledge the support of NIH grant EY01483 for this work.

References

1 Heller, J., Ostwald, T.J. and Bok, D. (1971) J. Cell. Biol. 48, 633–649
2 McConnell, D.G. (1975) J. Biol. Chem. 250, 1898–1906
3 Korenbrot, J.I., Brown, D.T. and Cone, R.A. (1973) J. Cell Biol. 56, 389–398
4 Hoffman, W.F., Norisuye, T. and Yu, H. (1977) Biochemistry 16, 1273–1278
5 Raubach, R.A., Nemes, P.P. and Dratz, E.A. (1974) Exp. Eye Res. 18, 1–12

6 Norisuye, T., Hoffman, W.F. and Yu, H. (1976) Biochemistry 15, 5678—5682
7 Worthington, C.R. (1973) Exp. Eye Res. 17, 487—501
8 McConnell, D.G. (1965) J. Cell Biol. 27, 459- 473
9 Perrin, F. (1936) J. Phys Radium 7, 1—11
10 Hagins, W.A. (1972) Annu. Rev. Biophys. Bioeng. 1, 131—158
11 Smith, Jr , H.G., Stubbs, G.W. and Litman, B.J (1975) Exp. Eye Res. 20, 211—217
12 Draper, N.R and Smith, H (1966) Applied Regression Analysis, Chap. 1, John Wiley and Sons, New York
13 Falk, G. and Fatt, P. (1969) J. Ultrastruct. Res. 28, 41—60
14 Sjostrand, F.S. (1949) J. Cell Comp. Physiol. 33, 383—397
15 Sjostrand, F.S. (1953) J. Cell Comp. Physiol. 42, 15—44
16 Heller, J., Ostwald, T.J. and Bok, D (1970) Biochemistry 9, 4884—4889
17 Blasie, J.K. (1972) Biophys. J. 12, 205—213
18 Poo, M.M. and Cone, R.A. (1973) Exp. Eye Res. 17, 503—510
19 Hagins, W.A. and Yoshikami, S. (1974) Exp. Eye Res. 18, 299—305
20 Mason, W.T., Fager, R.S. and Abrahamson, E.W. (1974) Nature 247, 562—563
21 Hendriks, Th., Daemen, F.J.M. and Bonting, S.L. (1974) Biochim. Biophys. Acta 345, 468—473
22 Weller, M., Virmaux, N. and Mandel, P. (1975) Nature 256, 68—70
23 Smith, Jr., H.G., Fager, R.S. and Litman, B.J. (1977) Biochemistry 16, 1399—1405
24 Houwink, R. (1958) Elasticity, Plasticity and Structure of Matter, p. 217, Dover, New York
25 Saito, N. and Ikeda, Y. (1951) J. Phys. Soc. Japan 6, 305—308
26 Moriguchi, S., Udagawa, K. and Hitotsumatsu, S. (1956) Mathematical Formulae (in Japanese), Vol. I., p. 54, Iwanami, Tokyo
27 Abramowitz, M. and Stegun, I.A. (1964) Handbook of Mathematical Functions, NBS Applied Mathematics Series 55, p. 555, U.S. Government Printing Office, Washington, D.C.